**THE EUROPEAN
PHYSICAL JOURNAL D**

Regular Article

Plasmid DNA damage induced by helium atmospheric pressure plasma jet[★]

Xu Han, William A. Cantrell, Erika E. Escobar[a], and Sylwia Ptasinska[b]

Radiation Laboratory and Department of Physics, University of Notre Dame, Notre Dame, IN 46556, USA

Abstract. A helium atmospheric pressure plasma jet (APPJ) is applied to induce damage to aqueous plasmid DNA. The resulting fractions of the DNA conformers, which indicate intact molecules or DNA with single- or double-strand breaks, are determined using agarose gel electrophoresis. The DNA strand breaks increase with a decrease in the distance between the APPJ and DNA samples under two working conditions of the plasma source with different parameters of applied electric pulses. The damage level induced in the plasmid DNA is also enhanced with increased plasma irradiation time. The reactive species generated in the APPJ are characterized by optical emission spectra, and their roles in possible DNA damage processes occurring in an aqueous environment are also discussed.

1 Introduction

The development of the atmospheric pressure plasmas, i.e., atmospheric pressure plasma jets (APPJs) and dielectric barrier discharges (DBDs), has driven plasma physics to an innovative interdisciplinary stage in which radiation physical chemistry and biomedicine have been synergized. Due to one of the most significant features of atmospheric pressure plasmas, namely that they can be used under ambient air conditions, elevated temperatures and costly complex vacuum systems can be avoided in contrast to traditional plasma sources. Therefore, this type of plasma source provides a desirable condition for treating temperature- and vacuum-sensitive biological samples [1].

There is a growing interest in the effects of the atmospheric pressure plasmas on living matter at the cellular level such as inducing cell apoptosis for cancer treatment [2–6], tissue sterilization and wound healing [7–15]. To explore these effects in more detail, an understanding of the roles of plasma species in a complex cell system was found to be essential [1,16–20]. Among all biomolecules, one of the most important is deoxyribonucleic acid (DNA), because it plays a key function in the storage of genetic information, which is passed to the next cell generation at each cellular division. Even relatively small amounts of

damaged DNA can lead to cell death; therefore, DNA can be considered a critical target of plasma radiation [4,21].

Since the APPJ contains multiple types of species, such as radicals, electrons, photons, and charged particles, direct plasma radiation on a target, e.g., a cancer cell, can cause ionization or excitation at the molecular level. In cells, these processes may initiate an event cascade that could lead to biological changes in DNA [21]. The individual roles of different APPJ species in inducing DNA damage was recently reported by Ptasinska et al. [22]. The authors stated that each type of APPJ species caused different damage levels in dry DNA with the excited and neutral reactive species contributing the most to DNA alteration [22]. Plasma irradiation can also affect DNA through an indirect pathway that is via interactions with solvated electrons and free radicals produced by the primary ionizing radiation in a medium containing DNA. This indirect action is considered a major contributor in the presence of water [21], e.g., when DNA is dissolved in aqueous solution. In such a scenario, the radiolysis of water plays a critical part in the rapid generation of oxidizing radical intermediates [21]. The cellular environment of DNA, however, is more complex due to the bound water, proteins and endogenous free-radical scavengers. For instance, sulfhydryl groups (-SH) generated naturally in a cell can decrease the damaging effects by reacting with free radicals [21]. Moreover, DNA as a part of chromatin [23] is bound to histone proteins, which behave as scavengers for destructive radicals generated by radiation [24]. The role of amino acids in the vicinity of DNA during plasma treatment was investigated previously, and it has been shown that the level of protection depends on the amount and type of amino

---

[★] Contribution to the Topical Issue "Nano-scale Insights into Ion-beam Cancer Therapy", edited by Andrey V. Solov'yov, Nigel Mason, Paulo Limão-Vieira, Malgorzata Smialek-Telega.

[a] *Present address*: Department of Physics and Astronomy, California State University at Long Beach, CA 90840, USA.

[b] e-mail: `sptasins@nd.edu`

acid [25]. Thus, the presence of other molecules around DNA may alter the consequence of radiation.

During plasma irradiation, an intact supercoiled (SC) structure of plasmid DNA can deform into a circular shape due to a single strand break (SSB) or into a linear shape due to a double strand break (DSB). If a SSB happens, one scission event occurs on one strand, and in the case of a DSB, the second cleavage is at or close to the same location as the first but on the other strand [26–28]. Typically, SSBs can be induced by hydrogen atom abstraction from the DNA sugar moiety, deoxyribose, that is triggered by an OH radical that can further react with oxygen to form a peroxy radical ($RO_2^\bullet$) [21,29]. Sugar damage can also occur in the presence of molecular oxygen, which reacts with sugar radicals to form phosphoglycolate along with the release of the base propenal (nucleobase-C_3H_3O) [30]. After the strand breaks, the release of torsional energy stored in the SC form of the DNA structure allows a conformational change from a supercoiled to an open circular form [31]. If the DNA molecule is under a localized attack by two or more OH radicals, a DSB may be produced, resulting in the formation of a linear polynucleotide [31]. DSBs can also be achieved in an alternative scenario, such as a hybrid attack. A hybrid attack is a combination of direct and indirect actions, where the OH radical is responsible for a scission at one site within about ten base pairs or less away from another direct damage location [21]. The DNA breakages have been shown to be reduced by adding a certain amount of OH radical scavengers, e.g., ethylenediaminetetraacetic acid-tris(hydroxymethyl)aminomethane (tris-EDTA) [27]. In addition to radicals, free electrons are also an important component of plasma, and they should be taken into account as a possible factor in DNA damage. It has been shown that bombardment of plasmid DNA with electrons in the range of 0–4 eV induces SSBs [32] and in the range of 3–15 eV induces both SSBs and DSBs with maximum damage occurring at 10 eV [33].

Since SSB and DSB formation in DNA molecules can be indicators of cell mortality [34], it is vital to precisely quantify these processes. The fundamental investigations of DNA damage induced by plasma can offer important information at the cellular level for further applications of plasma. Therefore, it is essential to gain a better understanding of the impact of plasma on plasmid DNA.

In this study, plasmid DNA in aqueous solution is treated by a helium APPJ at different distances and for various exposure times under two different working conditions of the plasma source. The degradation of the supercoiled form and the generation of SSBs and DSBs due to plasma irradiation were quantified.

2 Experimental setup and sample handling

A schematic diagram of the plasma source used is presented in Figure 1a. Two tubular brass electrodes with a 6 mm inner diameter were placed around a 20 cm long fused silica tube that had an inner diameter of 5 mm and a wall thickness of 0.5 mm. One of the two electrodes was grounded, and the other was connected to a high voltage
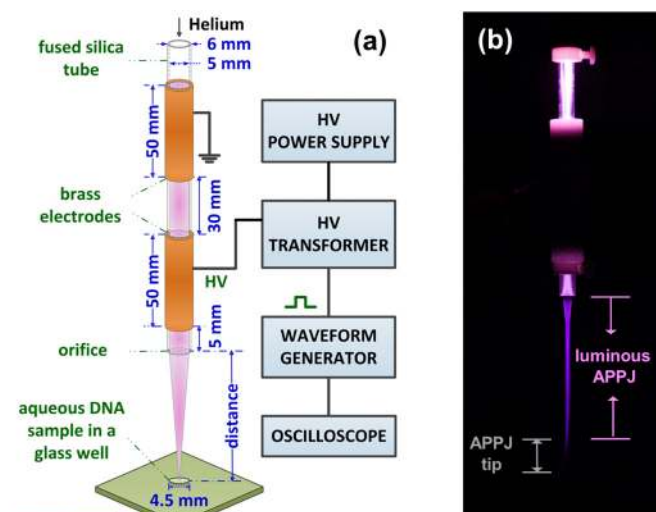

Fig. 1. The experimental setup. (a) A schematic diagram of the helium plasma source used for treating an aqueous DNA sample on a glass substrate. The sample was placed at different distances from the tube orifice. (b) A photograph of the plasma discharge inside the tube and the launched APPJ. The length of the luminous part of the jet is about 5–6 cm from the orifice with a helium gas flow of 4 L/min under the high-power plasma condition. The photograph was taken by a Canon EOS 5D Mark III camera with a 1/40 s exposure time.

(HV) transformer coupled to a custom-made HV power supply. The electrodes were separated by a gap of 3 cm along the fused silica tube.

Under the first working condition, a square pulse with a 5 μs width and a repetition rate of 2.5 kHz was produced by a pulse waveform generator (80 MHz Function/Arbitrary Waveform Generator, 33 250 A, Agilent Tech.) which was coupled to the HV transformer and applied to the powered electrode. Plasma was ignited between the two electrodes in a helium stream flowing through the tube. In this study, the flow rate was regulated by a flow controller (MASS-VIEW flow regulator, MV-394-He, Bronkhorst High-tech) and was set to be 4 L/min. The amplitudes of the voltage and current were monitored at the powered electrode and displayed values of 7 kV and 10 mA, respectively, on an oscilloscope (Tektronix TDS2004B, 60 MHz). These readings were measured by using the voltage (Tektronix TCP A300) and current (Tektronix P6015A) probes. Assuming a square wave the pulse energy and the average input power were estimated to be 0.35 mJ and 0.88 W, respectively.

Under the second working condition, another custom-made, high voltage power supply was used with a square pulse of 100 μs width at a frequency of 1.5 kHz. The amplitudes of voltage and current on the powered electrode were recorded as 10.8 kV and 110 mA, respectively. The same flow rate of helium (4 L/min) was applied. Assuming a square wave the pulse energy and the average input power were estimated to be 118.8 mJ and 178.2 W, respectively. Hereafter, the condition of the plasma source with the first electrical setting is called a low-power plasma

condition and with the second one is called a high-power plasma condition.

For both plasma source parameter settings, the dielectric barrier discharge is visible not only between the two electrodes but also as a jet (the APPJ) that projected a few centimeters in length out of the fused silica tube into the open atmosphere (Fig. 1b).

The pUC18 plasmid DNA (2686 base pairs) extracted from *Escherichia coli (E. coli)* was prepared as described previously [35]. Each sample was diluted in 15 μL of deionized (DI) water to contain 100 ng DNA. The diluted sample was injected into a well (20 μL maximum volume, diameter of 4.5 mm) on the surface of a boron silicate glass. The glass substrate was placed on an adjustable sample holder, which allowed varying of the distance between the orifice and the sample (Fig. 1a). After irradiation, the majority of the solution was pipetted out. The remaining DNA solution was collected by adding DI water or PBS (Phosphate Buffered Saline) to the glass well and pipetting out.

To quantify and qualify the DNA damage induced by plasma radiation, the electrophoresis technique was applied using a gel set (Bio-Rad Laboratories, Inc.). Agarose powder (Bio-Rad Laboratories, Inc., USA) was dissolved in 1 X TBE buffer (Tris/ boric acid/ EDTA, Bio-Rad Laboratories, Inc., USA) to form 0.8% agarose gel that was pre-stained with a fluorescent dye (SYBR Green I Nucleic Acid Stain, 10 000 X concentration in DMSO, Lonza, USA). The samples were electrophoresed on the prepared agarose gel at 70 V in 1X TBE running buffer. After the electrophoresis was completed, the DNA bands for different conformations (SC, SSB and DSB) were visualized by a gel imager (Molecular imager Gel Doc XR + System, Bio-Rad Laboratories, Inc.) upon UV light exposure. A specialized software (Quantity One, 1-D Analysis Software, Bio-Rad Laboratories, Inc.) was used to display images and quantify the fluorescence intensity of each band. The fluorescence intensity indicated the amount of a particular conformation of DNA that was present in the sample. By estimating the ratio of the fluorescence intensity of each type of conformers to that of all the conformers within each irradiated sample or within each control sample and then by averaging over a few samples treated at the same conditions, the damage level induced by plasma as a fraction of the total plasmid DNA in solution was determined.

3 Results and discussion

Figure 2 displays a representative gel image for the DNA samples treated by the APPJ for 20 s at a distance of 4.5–6.5 cm (sample No. 4–8). In addition to plasma irradiated samples, three types of control samples (sample No. 1–3) were used: (1) the tube control DNA is the DNA stock solution and directly loaded into the gel; (2) the glass substrate control is diluted DNA placed into a glass well that is then collected and loaded into the gel; and (3) the flow control is diluted DNA that is placed onto the glass
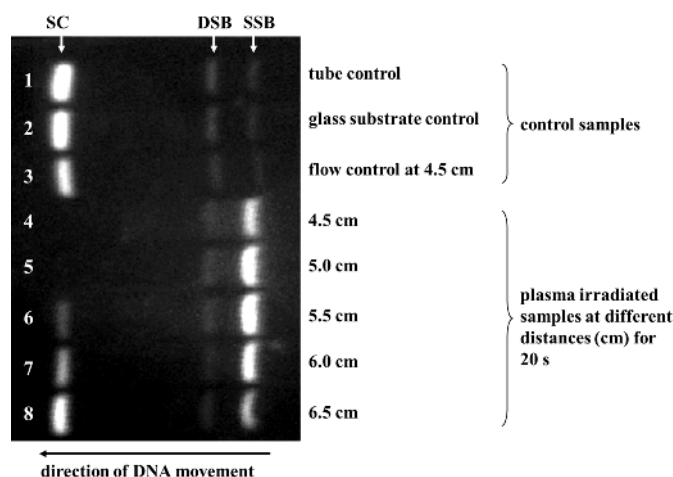

Fig. 2. A representative agarose gel image of the control and plasma-treated DNA samples. The image shows a distribution of different bands, which correspond to supercoiled (SC), double-strand break (DSB), and single-strand break (SSB) DNA conformers. A brighter band indicates a larger amount of DNA conformers.

substrate, treated with pure helium flow for 20 s at a distance of 4.5 cm, and then collected and loaded into the gel. By comparing the control samples with the plasma treated samples, external factors that could possibly induce damage (e.g., substrate and gas flow) are monitored offering accurate insight into the role of plasma as the main contributor to DNA damage. All control samples show low DNA damage, which is less than 5%.

Since the species distribution in the plasma jet depends on the distance from the orifice [22,36], it is important to investigate DNA damage at different positions. Figure 3a presents the conformer fraction of the total plasmid DNA (the sum of SC, DSB and SSB amount) as a function of the distance (1–15 cm) from the orifice after plasma treatment for 20 s under the low-power plasma condition. When the specimen is at farther distances from the orifice (9–16 cm), the DNA sample remains mainly in the SC form (>93%) after plasma irradiation with a very small amount of SSBs (<5%) and DSBs (<3%) observed. This minor damage is due to the tendency of the radicals to diffuse into the atmosphere at long distances from the APPJ, which will be shown later from the optical emission spectra.

As the distance to the orifice is decreased to 8 cm, the yield of the SC form shows a slight degradation with a corresponding increase in SSBs. Between 5.5 and 8 cm, a rapid alteration of the SC structures occur along with formation of SSBs. The large error bars for the data obtained in this region are most likely due to the relatively unstable nature of the APPJ tip. The length of the jet and its tip position may also slightly vary during discharges contributing to these error bars. At distances less than 5 cm, the SC fraction decreases below 5%, and the SSB fraction is above 91%. The DSB fraction, however, does not vary significantly within these distances; it is relatively constant at less than 5%. These results reveal that the generation of SSBs is enhanced at shorter distances,
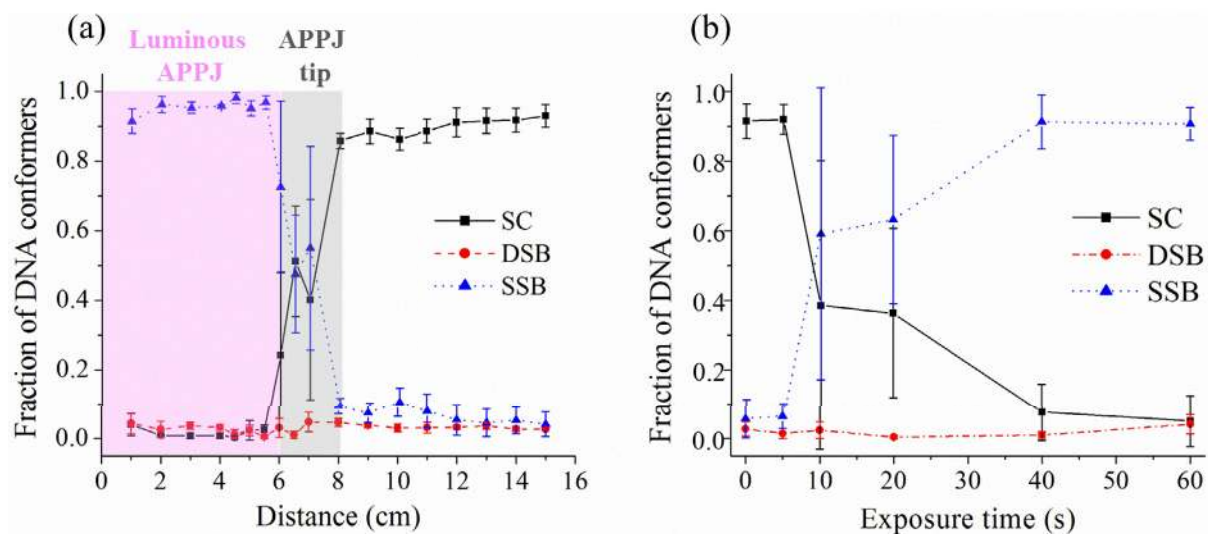
Fig. 3. Fraction of SC, DSB, and SSB DNA conformers induced by APPJ radiation under the low-power plasma condition (a) at various distances for a plasma irradiation time of 20 s and (b) with different irradiation times at a distance of 6 cm. Regions corresponding to the luminous part and the tip of APPJ are highlighted in light pink and light grey, respectively. Each data point is obtained from the average of at least three independent trials.

indicating that more SC DNA molecules are damaged and transformed into the circular form. It is also shown that no apparent linear conformers are formed because there is only slight variation in the fraction of DSBs.

The second variable explored with respect to APPJ interaction with DNA samples is the duration of plasma irradiation. In Figure 3b, the damage effect is indicated in terms of the fraction of DNA conformers as a function of plasma irradiation time at a distance of 6 cm from the orifice. At this distance, the APPJ is still in direct contact with the DNA sample and some amount of intact DNA molecules is still present; therefore, the effect of exposure time can be seen at this distance. If a shorter distance had been chosen, the time effect could not have been investigated because after 20 s of irradiation most of the DNA molecules are already damaged (Fig. 3). If a farther distance had been chosen, the APPJ would not have been in contact with the sample. As irradiation time increases from 5 to 60 s, the SC fraction decreases from approximately 92% to 5%, while the SSB yield follows the opposite trend increasing from around 6% to 91%. The production of DSBs remains constant at approximately 4% during all irradiation times. It is interesting to note that the process of SSB formation occurs very fast: the exposure of only 10 s results in the deformation of around 60% SC into SSB conformers. After 40 s of treatment, the SSB fraction becomes the clearly dominant portion (above 90%) of the total DNA conformers in the sample. It is reasonable to view this trend as a result of a direct plasma effect, meaning that APPJ reactive species, which are impinged to the liquid, cause strand breaks by attacking the phosphodiester bonds or nucleobases directly. Alternatively, it could be the result of an indirect plasma effect, meaning a cascade of chemical reactions in the liquid environment initiated by APPJ reactive species. Smaller error bars are observed in the samples irradiated above 40 s,

which is a sufficient time for the APPJ reactive species to induce damage to a large number of DNA molecules in the sample.

The same experimental procedure was also carried out under the high-power plasma condition. Figure 4 displays the following results: the fraction of three DNA conformers as a function of distance (Fig. 4a) and time (Fig. 4b) of APPJ treatment.

Figure 4a shows a relatively constant production (80%) of SSB conformers at distances up to 3 cm that corresponds to a luminous part of the APPJ. The length of the APPJ under the high-power plasma condition is about half as long as that for the APPJ under the low-power plasma condition. Much higher fluctuations of data are observed for distances greater than 3 cm (Fig. 4a). Interestingly, DSBs are generated in DNA samples that are located at short distances to the orifice of the plasma source tube that are not observed in Figure 3a. As it was reported previously, electrical parameters of the plasma source have a significant influence on the formation and characteristics of plasma jets [36,37].

From a comparison of the time-dependent trends for the two different power conditions of the plasma source, DSBs are induced at shorter exposure times (>10 s), as seen in Figure 4b, implying that a larger number of reactive species are formed under the high-power plasma condition. A similar trend of the increase in the DSB fraction with exposure time was also observed in the work performed by Stypczynska et al. [25].

To characterize the reactive species generated in the APPJ, optical emission spectra (OES) were taken in the range of 280 to 800 nm by a fiber optic spectrometer (USB2000-UV-VIS, Ocean Optics, Inc.). Due to a possibility that DSBs and large amounts of radicals are produced, all of the present OES were obtained under the high-power plasma condition. As shown in Figure 5,
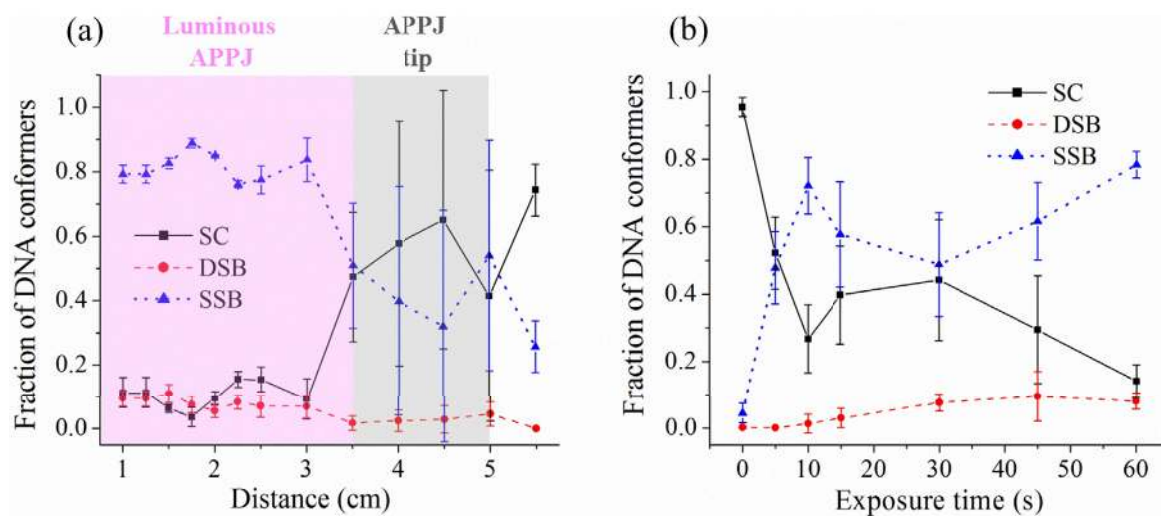
Fig. 4. Fraction of SC, DSB, and SSB DNA conformers induced by APPJ radiation under the high-power plasma condition (a) at various distances for a plasma irradiation of 30 s and (b) with different irradiation times at a distance of 2.5 cm. Regions corresponding to the luminous part and the tip of APPJ are highlighted in light pink and light grey, respectively. Each data point is obtained from the average of at least three independent trials.
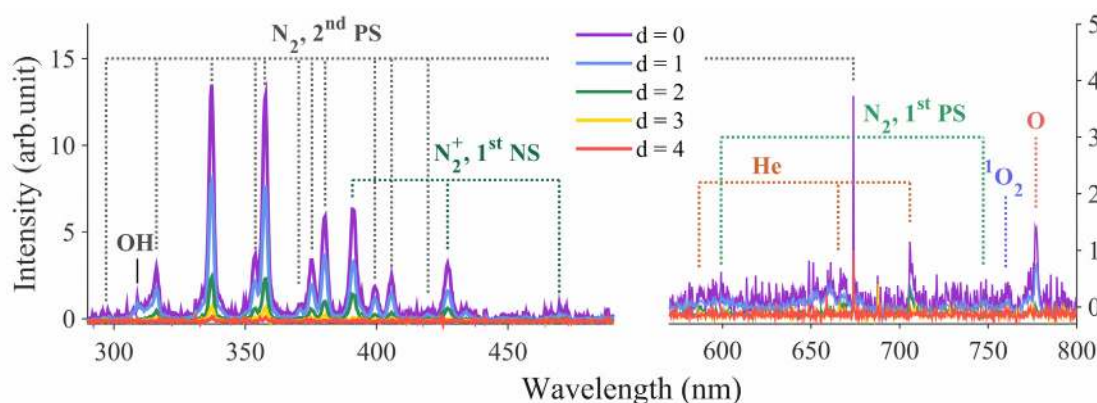

Fig. 5. The optical emission spectra of APPJ at distances (d), varying from 0 to 4 cm with a 3.5 L/min helium flow rate, at wavelengths of 280–800 nm taken under the high-power plasma condition.

the emission peaks contribute to several groups with the second positive system (2nd PS) of molecular nitrogen (N_2) and the first negative system (1st NS) of ionic nitrogen (N_2^+) as the most dominant bands [22,25]. The first positive system (1st PS) of N_2 is observed in the range of 750 and 600 nm. The presence of these nitrogen species is caused by the higher energy state of molecular or ionic nitrogen molecules excited by discharged electrons [38]. Hydroxyl (OH) radical emission peak is recorded at 309 nm, which may result from the collision of H_2O^+ with electrons (H_2O^+ is produced from the reaction of water molecules with metastable helium atoms or metastable helium dimers) [39]. The emission peak of atomic oxygen (O) and the oxygen molecule in the singlet state ($^1O_2$) appear near the infrared region at 777 nm and 762 nm, respectively. The atomic oxygen may be generated from the collisions of molecular oxygen gas with either electrons or nitrogen molecules, and then it can be converted into O_2 and O_3 due to its high reactivity [40]. The existence of O and $^1O_2$ can offer the

potential oxidative stress that facilitates DNA breakage in the cell [41,42]. The emission bands of He at 587 nm, 668 nm, and 706 nm indicate the excitation process during APPJ ignition [39].

By placing the optical sensor at different distances from the orifice, a variation in intensity for several emission peaks is observed (Fig. 5). As the distance changes from 4 to 0 cm, all peaks become more prominent, indicating a higher density of generated species. At a distance of 4 cm, the whole spectrum remains close to zero intensity due to short lifetimes and diffusion of these species.

The quenching of OH radical signals at larger distances in the OES (Fig. 5) indicates a decreasing density of OH radicals in the gas phase, and thus their impact on the DNA molecules is reduced. However, when water molecules are electronically excited during the interaction with radiation, the excited state of the water molecule (H_2O^*) can be generated [30]. After its production, the H_2O^* state undergoes dissociation into H and OH radicals [30].

Moreover, other reactive species formed by the species present in an APPJ, e.g., solvated electrons which are powerful reductants [30], can be also indirectly involved in DNA damage in a liquid environment. Alternatively, when oxygen molecules diffuse into the aqueous solution, they react with solvated electrons to form the highly reactive superoxide radical ($O_2^{\bullet-}$) [43]. The superoxide radical can then be spontaneously converted into hydrogen peroxide (H_2O_2) by the superoxide dismutation reaction [43], which can be followed by the generation of OH radicals through the Fenton reaction [40]. In addition, if the solvated electrons are captured by organic acceptor molecules (e.g., nucleobases), radical anions will be produced, which can be oxidized rapidly by O_2, with the formation of superoxide radicals [44]. A period DNA strand breaks can also be caused by $^1O_2$ species produced in the APPJ when it diffuses into the water environment [42]. Additionally, due to the collisions of N_2 and O_2 in the APPJ both NO and NO_2 species can be generated [45]. Though NO species are probably insufficiently reactive to cause DNA damage directly [46], the further reaction products of NO, such as HNO_2 [43,45] and $OONO^-$ [40] can contribute to the nitration and deamination of DNA and thus lead to strand breaks [46–51].

4 Conclusions

Strand breaks (mainly SSBs) in aqueous plasmid DNA samples were induced by a helium atmospheric pressure plasma jet. The contribution to DNA damage of variations in both distance from the plasma tube and exposure time has been discussed with respect to two different electrical parameter settings of the plasma source. The damage level was shown to rise dramatically when the sample was within the jet tip region. A high fraction of SSBs was obtained after only a short duration of plasma treatment, which supports the effectiveness of plasma for inducing DNA scissions. A low level of DSB damage was observed mainly under the high-power plasma source condition. Possible fast chemical reactions and diffusion processes between reactive radicals in the jet and the liquid environment may be largely responsible for the generation of the strand breaks. Thus, the detailed determination of the species types generated in liquid during plasma irradiation will be essential to further explore the mechanisms of DNA damage. Studies on the interactions between plasma and aqueous DNA molecules can bring insight to the radiation scenario for a cellular system and thus be critical to the development of plasma medical applications.

References

1. T. von Woedtke, S. Reuter, K. Masur, K.-D. Weltmann, Phys. Rep. **530**, 291 (2013)
2. I.E. Kieft, J.L.V. Broers, V. Caubet-Hilloutou, D.W. Slaaf, F.C.S. Ramaekers, E. Stoffels, Bioelectromagnetics **25**, 362 (2004)
3. G. Fridman, A. Shereshevsky, M.M. Jost, A.D. Brooks, A. Fridman, A. Gutsol, V. Vasilets, G. Friedman, Plasma Chem. Plasma Proc. **27**, 163 (2007)
4. G.J. Kim, W. Kim, K.T. Kim, J.K. Lee, Appl. Phys. Lett. **96**, 021502 (2010)
5. M. Vandamme, E. Robert, S. Lerondel, V. Sarron, D. Ries, S. Dozias, J. Sobilo, D. Gosset, C. Kieda, B. Legrain, J.-M. Pouvesle, A. Le Pape, Int. J. Cancer **130**, 2185 (2012)
6. X. Han, M. Klas, Y. Liu, M. Sharon Stack, S. Ptasinska, Appl. Phys. Lett. **102**, 233703 (2013)
7. T.C. Montie, K. Kelly-Wintenberg, J.R. Roth, IEEE Trans. Plasma Sci. **28**, 41 (2000)
8. M. Moisan, J. Barbeau, M.-C. Crevier, J. Pelletier, N. Philip, B. Saoudi, Pure Appl. Chem. **74**, 349 (2002)
9. M. Laroussi, Plasma Process. Polym. **2**, 391 (2005)
10. G. Fridman, M. Peddinghaus, M. Balasubramanian, H. Ayan, A. Fridman, A. Gutsol, A. Brooks, Plasma Chem. Plasma Proc. **26**, 425 (2006)
11. T. Sato, T. Miyahara, A. Doi, S. Ochiai, T. Urayama, T. Nakatani, Appl. Phys. Lett. **89**, 073902 (2006)
12. G. Fridman, G. Friedman, A. Gutsol, A.B. Shekhter, V.N. Vasilets, A. Fridman, Plasma Process. Polym. **5**, 503 (2008)
13. T. Sato, O. Furuya, K. Ikeda, T. Nakatani, Plasma Process. Polym. **5**, 606 (2008)
14. G. Isbary, G. Morfill, H.U. Schmidt, M. Georgi, K. Ramrath, J. Heinlin, S. Karrer, M. Landthaler, T. Shimizu, B. Steffes, W. Bunk, R. Monetti, J.L. Zimmermann, R. Pompl, W. Stolz, Br. J. Dermatol. **163**, 78 (2010)
15. J. Heinlin, G. Isbary, W. Stolz, G. Morfill, M. Landthaler, T. Shimizu, B. Steffes, T. Nosenko, J. Zimmermann, S. Karrer, J. Eur. Acad. Dermatol. Venereol. **25**, 1 (2011)
16. M.G. Kong, G. Kroesen, G. Morfill, T. Nosenko, T. Shimizu, J. van Dijk, J.L. Zimmermann, New J. Phys. **11**, 115012 (2009)
17. S. Cheruthazhekatt, M. Èernák, P. Slavîeek, J. Havel, J. Appl. Biomed. **8**, 55 (2010)
18. C.-H. Kim, J.H. Bahn, S.-H. Lee, G.-Y. Kim, S.-I. Jun, K. Lee, S.J. Baek, J. Biotechnol. **150**, 530 (2010)
19. H.J. Ahn, K. Il Kim, G. Kim, E. Moon, S.S. Yang, J.-S. Lee, PLoS One **6**, e28154 (2011)
20. G. Park, Y.H. Ryu, Y.J. Hong, E.H. Choi, H.S. Uhm, Appl. Phys. Lett. **100**, 063703 (2012)
21. S. Lehnert, *Biomolecular Action of Ionizing Radiation*, 1st edn. (Taylor & Francis Group, New York, 2008)
22. S. Ptasinska, B. Bahnev, A. Stypczynska, M. Bowden, N.J. Mason, N.S.J. Braithwaite, Phys. Chem. Chem. Phys. **12**, 7779 (2010)
23. K. Luger, R.K. Richmond, D.F. Sargent, T.J. Richmond, A.W. Mader, Nature **389**, 251 (1997)
24. I. Radulescu, K. Elmroth, B. Stenerlöw, B. Stenerlo, Radiat. Res. **161**, 1 (2004)
25. A. Stypczynska, S. Ptasinska, B. Bahnev, M. Bowden, N.S.J. Braithwaite, N.J. Mason, Chem. Phys. Lett. **500**, 313 (2010)

26. X. Yan, F. Zou, X.P. Lu, G. He, M.J. Shi, Q. Xiong, X. Gao, Z. Xiong, Y. Li, F.Y. Ma, M. Yu, C.D. Wang, Y. Wang, G. Yang, Appl. Phys. Lett. **95**, 083702 (2009)

27. D. O'Connell, L.J. Cox, W.B. Hyland, S.J. McMahon, S. Reuter, W.G. Graham, T. Gans, F.J. Currell, Appl. Phys. Lett. **98**, 043701 (2011)

28. H. Kurita, T. Nakajima, H. Yasuda, K. Takashima, A. Mizuno, J.I.B. Wilson, S. Cunningham, Appl. Phys. Lett. **99**, 191504 (2011)

29. B. Halliwell, J.M.C. Gutteridge, *Free Radicals in Biology and Medicine*, 1st edn. (Oxford University Press, New York, 1985)

30. *Radiation Chemistry: From Basics to Applications in Material and Life Sciences*, edited by M. Spotheim-Maurizot, M. Mostafavi, T. Douki, J. Belloni, 1st edn. (EDP Sciences, Les Ulis, 2008)

31. C.S. Lengsfeld, T.J. Anchordoquy, J. Pharm. Sci. **91**, 1581 (2002)

32. F. Martin, P. Burrow, Z. Cai, P. Cloutier, D. Hunting, L. Sanche, Phys. Rev. Lett. **93**, 068101 (2004)

33. B. Boudaiffa, P. Cloutier, D. Hunting, M.A. Huels, L. Sanche, Science **287**, 1658 (2000)

34. E.L. Alpen, *Radiation Biophysics*, 1st edn. (Prentice-Hall, Inc., 1990)

35. S. Purkayastha, J.R. Milligan, W.A. Bernhard, J. Phys. Chem. B **109**, 16967 (2005)

36. A. Begum, M. Laroussi, M.R. Pervez, AIP Adv. **3**, 062117 (2013)

37. Q. Xiong, X. Lu, K. Ostrikov, Z. Xiong, Y. Xian, F. Zhou, C. Zou, J. Hu, W. Gong, Z. Jiang, Phys. Plasmas **16**, 043505 (2009)

38. F. Clément, E. Panousis, A. Ricard, E. Lecoq, J.-F. Loiseau, B. Held, J. Phys. Conf. Ser. **207**, 012007 (2010)

39. Z. Navrátil, R. Brandenburg, D. Trunec, A. Brablec, P. St'ahel, H.-E. Wagner, Z. Kopecký, Plasma Sources Sci. Technol. **15**, 8 (2006)

40. A. Fridman, *Plasma Chemistry*, 1st edn. (Cambridge University Press, New York, 2008)

41. B. Van Houten, V. Woshner, J.H. Santos, DNA Repair (Amst) **5**, 145 (2006)

42. L.-O. Klotz, K.-D. Kröncke, H. Sies, Photochem. Photobiol. Sci. **2**, 88 (2003)

43. Y. Yang, Y.I. Cho, A. Fridman, *Plasma Discharge in Liquid: Water Treatment and Applications*, 1st edn. (CRC Press, New York, 2012)

44. *Effects of Ionizing Radiation on DNA*, edited by J. Huttermann, W. Kohnlein, R. Teoule, A.J. Bertinchamps, 1st edn. (Springer-Verlag Berlin Heidelberg, New York, 1978)

45. P. Bruggeman, C. Leys, J. Phys. D **42**, 053001 (2009)

46. B. Halliwell, Mutat. Res. **443**, 37 (1999)

47. S. Tamir, S. Tannenbaum, Biochim. Biophys. Acta **1**, F31 (1996)

48. M.J. Juedes, G.N. Wogan, Mutat. Res. **349**, 51 (1996)

49. T. De Rojas-Walker, S. Tamir, H. Ji, J.S. Wishnok, S.R. Tannenbaum, Chem. Res. Toxicol. **8**, 473 (1995)

50. J.P. Spencer, J. Wong, A. Jenner, O.I. Aruoma, C.E. Cross, B. Halliwell, Chem. Res. Toxicol. **9**, 1152 (1996)

51. E. Felley-Bosco, Cancer Metastasis Rev. **17**, 25 (1998)